THE JOURNAL OF BIOLOGICAL CHEMISTRY VOL. 283, NO. 9, pp. 5466–5476, February 29, 2008
Printed in the U.S.A.

S-Phase-specific Activation of PKCα Induces Senescence in Non-small Cell Lung Cancer Cells*[S]

Received for publication, September 10, 2007, and in revised form, December 18, 2007 Published, JBC Papers in Press, December 26, 2007, DOI 10.1074/jbc.M707576200

Jose L. Oliva[‡§1,2], **M. Cecilia Caino**[‡1], **Adrian M. Senderowicz**[§], **and Marcelo G. Kazanietz**[‡3]

From the [‡]*Department of Pharmacology and Institute for Translational Medicine and Therapeutics, University of Pennsylvania School of Medicine, Philadelphia, Pennsylvania 19104-6160 and the* [§]*CDER, Food and Drug Administration, Silver Spring, Maryland 20993*

Protein kinase C (PKC) has been widely implicated in positive and negative control of cell proliferation. We have recently shown that treatment of non-small cell lung cancer (NSCLC) cells with phorbol 12-myristate 13-acetate (PMA) during G_1 phase inhibits the progression into S phase, an effect mediated by PKCδ-induced up-regulation of the cell cycle inhibitor $p21^{Cip1}$. However, PMA treatment in asynchronously growing NSCLC cells leads to accumulation of cells in G_2/M. Studies in post-G_1 phases revealed that PMA induced an irreversible G_2/M cell cycle arrest in NSCLC cells and conferred morphological and biochemical features of senescence, including elevated SA-β-Gal activity and reduced telomerase activity. Remarkably, this effect was phase-specific, as it occurred only when PKC was activated in S, but not in G_1, phase. Mechanistic analysis revealed a crucial role for the classical PKCα isozyme as mediator of the G_2/M arrest and senescence, as well as for inducing $p21^{Cip1}$ an obligatory event for conferring the senescence phenotype. In addition to the unappreciated role of PKC isozymes, and specifically PKCα, in senescence, our data introduce the paradigm that discrete PKCs trigger distinctive responses when activated in different phases of the cell cycle via a common mechanism that involves $p21^{Cip1}$ up-regulation.

Activation of protein kinase C (PKC)[4] with phorbol esters and related natural compounds causes an array of effects on differentiation, mitogenesis, survival, apoptosis, and transformation. The diverse effects of phorbol esters both in normal and cancerous cells is due to the existence of numerous intracellular effectors, of which PKC isozymes have been the most widely characterized. The PKC family comprises 3 subfamilies that include 10 structurally related phospholipid-dependent serine/threonine kinases (1, 2). Members of the classical cPKC (α, βI, βII, and γ) and the novel nPKC (δ, ϵ, η, and θ) subfamilies are activated by phorbol esters and their cellular analogue, the second messenger diacylglycerol, which leads to redistribution (translocation) of the enzymes from cytosol to intracellular membrane compartments, where they phosphorylate specific substrates. The marked heterogeneity in the signaling events and cell type-specific responses triggered by phorbol esters could be explained by the distinctive pattern of expression and intracellular localization of PKC isozymes and their substrates, which ultimately results in selective pathway activation.

One of the paradigms that best exemplifies the functional versatility of PKC isozymes is the regulation of the cell cycle machinery. It became evident in the last years that PKCs can impact on the cell cycle both in positive and negative manners with a strict degree of cell type and isozyme specificity. PKC isozymes have been shown to regulate the progression of cells from G_1 to S phase as well as with the transition from G_2 to M phase (3) via transcriptional, translational, and post-translational mechanisms. PKCs control the activity of cyclin-Cdk complexes in G_1 by modulating the expression of cyclins and Cdk inhibitors (4, 5). For example, early studies in vascular endothelial cells showed dual growth stimulatory or inhibitory roles for PKCs depending on which phase in the cell cycle PKC becomes activated. In HUVEC cells phorbol esters potentiate growth factor mitogenic activity when added in early G_1 phase, but they inhibit DNA synthesis when added in late G_1 phase (6). In NIH 3T3 cells, PKCα and PKCϵ enhance cell cycle progression and proliferation by stimulating cyclin D1 transcription (7). On the other hand, PKCη inhibits cdk2 activity in human keratinocytes, and overexpression of either PKCη or PKCδ, but not PKCα, leads to G_1 arrest and differentiation (8, 9). In several cell types, the PKC activator phorbol 12-myristate 13-acetate (PMA) up-regulates Cdk inhibitors $p21^{Cip1}$ and/or p27 (10, 11). These contrasting effects ultimately impact on the status of Rb phosphorylation, the expression of E2F-regulated genes, and the biological outcome. Several studies have also established key roles for PKC isozymes in G_2. For example, PKCβII activation was required for entry into mitosis in HL60 promyelocytic leukemia cells (12), whereas PMA was shown to induce G_2 arrest by suppression of cdc2 kinase activity in vascular endothelial cells (13). Based on this complexity, it is not surprising that both PKC activators (such as bryostatins or phorbol esters)

* This work was supported by Grants CA-89202 and CA-92537 from the National Institutes of Health (to M. G. K.). The costs of publication of this article were defrayed in part by the payment of page charges. This article must therefore be hereby marked "*advertisement*" in accordance with 18 U.S.C. Section 1734 solely to indicate this fact.

[S] The on-line version of this article (available at http://www.jbc.org) contains supplemental Figs. S1–S4.

[1] Both authors contributed equally to this work.

[2] To whom correspondence may be addressed: Unidad de Biología Celular, Centro Nacional de Microbiología, Instituto de Salud Carlos III, Carretera Majadahonda-Pozuelo, Km. 2 Majadahonda-28220 Madrid, Spain. E-mail: jloliva@isciii.es.

[3] To whom correspondence may be addressed: Dept. of Pharmacology, University of Pennsylvania School of Medicine, 816 Biomedical Research Bldg. II/III, 421 Curie Blvd., Philadelphia, PA 19104-6160. E-mail: marcelo@spirit.gcrc.upenn.edu.

[4] The abbreviations used are: PKC, protein kinase C; DAPI, 4′,6-diamidino-2-phenylindole; NSCLC, non-small cell lung cancer; PBS, phosphate-buffered saline; PMA, phorbol 12-myristate 13-acetate; HU, hydroxyurea; MOI, multiplicity of infection; SA-β-Gal, senescence-associated β-galactosidase.

and PKC inhibitors (such as the PKCβ inhibitor enzastaurin) are in clinical trials for a number of neoplasias (14–17). Because of the contrasting effects of PKC isozymes on cell cycle regulation, a thorough understanding of these mechanisms is essential for the rational design of PKC modulators with anti-cancer activity.

Lung cancer is one of the most common forms of cancers worldwide and the major cause of cancer-related mortality. Non-small cell lung carcinoma (NSCLC), the most frequent type of lung cancer, is treated in early stages mainly with surgery and radiotherapy, whereas advanced stages receive combination chemotherapy or radiation therapy (18). Unfortunately, the marked resistance to the various therapies accounts for the high lethality (19). Studies in the last years have proposed PKC isozymes, such as PKCα, as targets for NSCLC therapy. However, a PKCα-specific antisense oligonucleotide (ISIS 3521/LY900003) showed slight or no benefit in NSCLC patients, either alone or in combination with other chemotherapeutic agents (20). This is not unexpected since PKCα, like other PKCs, has been shown to be either growth inhibitory or pro-apoptotic in various cancer cell models (21–23). One may speculate that activators of growth inhibitory PKCs rather than PKC inhibitors could have therapeutic benefits for lung cancer, as demonstrated for other types of cancers. It is evident that a deeper knowledge of the roles of individual PKC isozymes in lung cancer would be needed to rationalize the use of PKC as a therapeutic target.

Our recent studies have established that treatment of NSCLC cells with phorbol ester in early G_1 impairs the progression through S phase, and we have identified PKCδ as the PKC responsible for this effect. PKCδ-induced G_1 arrest is mediated through the transcriptional up-regulation of the cell cycle inhibitor $p21^{Cip1}$ (24). However, as shown in the present article, the paradox seems to be more complex, because in asynchronously growing NSCLC cells phorbol esters lead to the accumulation of cells in G_2/M, thus suggesting multiple points of regulation in the cell cycle by PKCs. A more detailed analysis revealed that activation of PKC in late G_1-early S leads to a delay in the progression through S phase and irreversible arrest of cells in G_2/M, followed by the appearance of a senescence phenotype. Both G_2/M arrest and senescence depend on the up-regulation of $p21^{Cip1}$, but strikingly these effects are mediated by PKCα rather than PKCδ. Exploiting this irreversible induced growth arrest of lung cancer cells in response to PKCα activation may have significant therapeutic implications.

EXPERIMENTAL PROCEDURES

Materials—Cell culture media was purchased from Invitrogen (Carlsbad, CA). PMA was obtained from LC Laboratories (Woburn, MA). The pan-PKC inhibitor GF109203X (bisindolylmaleimide I) was from BIOMOL Research Laboratories Inc. (Plymouth Meeting, PA). Gö6976 and rottlerin were purchased from Alexis (San Diego, CA). Propidium iodide, DAPI, and hydroxyurea were from Sigma-Aldrich.

Cell Culture—H358 and H441 lung bronchoalveolar adenocarcinoma cells were obtained from ATCC (Manassas, VA). H322 lung bronchoalveolar carcinoma cells were kindly provided by Dr. Steven Albelda (University of Pennsylvania School of Medicine). Cells were cultured in RPMI 1640 medium supplemented with 10% fetal bovine serum, penicillin (100 units/ml), streptomycin (100 μg/ml), and L-glutamine (2 mM) at 37 °C in a humidified 5% CO_2 atmosphere. For synchronization at the G_1/S boundary, cells were cultured in normal medium for 24 h, serum-starved for 24 h, and then treated with 1 mM hydroxyurea (HU) in complete medium. For synchronization in G_0, cells were serum-starved for 48 h, and released from G_0 by the addition of serum.

Cell Proliferation and Cell Cycle Analysis—Cells (2×10^5) were seeded in 60-mm dishes in triplicate and synchronized at the G_1/S boundary with HU as described above. Upon release by extensive washing, cells were treated with PMA or vehicle for different times. After extensive washing to remove the PMA, complete growth medium was added. Cells were trypsinized at different intervals and counted with a hemocytometer. Proliferation was assayed by [^{3}H]thymidine incorporation. Briefly, 24, 48, or 72 h after PMA treatment cells were pulse-labeled with 3 μCi/ml of [*methyl*-^{3}H]thymidine (Amersham Biosciences) for 3 h, followed by trichloroacetic acid precipitation and scintillation counting. For determination of cell cycle profile, cells were stained with propidium iodide (0.1 mg/ml) and analyzed by flow cytometry, as previously described (24).

Adenoviral Infections—Cells were infected with replication-deficient adenoviruses (AdV) for either PKCα or LacZ as a control (23, 25) 4 h (MOI, 100 pfu/cell) in serum-free RPMI 1640 medium. After removal of the AdV by extensive washing, cells were incubated in complete medium for 20 h. Expression of PKCα was readily detected 24 h after infection and remained stable for several days (data not shown). Amplification of AdVs was carried out in HEK293 cells. Titers of viral stocks were normally higher than 1×10^9 pfu/cell.

Western Blot Analysis—Cells were lysed in a buffer containing 50 mM Tris-HCl, pH 6.8, 10% glycerol, 2% SDS, and 5% β-mercaptoethanol. Cell extracts (20 μg of protein/lane) were subject to SDS-PAGE and transferred to polyvinylidene difluoride membranes (Millipore, Bedford, MD). After blocking with 5% milk in 0.1% Tween 20/PBS, membranes were incubated with the primary antibody. The following first antibodies were used: anti-PKCα and anti-cyclin D1 (Upstate Biotechnology Inc., Lake Placid, NY); anti-cyclin A1, anti-cyclin B1, anti-cyclin E, anti-E2F-1, anti-p27, anti PKCε and anti-PCNA (Santa Cruz Biotechnology Inc., Santa Cruz, CA); anti-$p21^{Cip1}$, anti-ATF-2 and anti-PKCδ (Cell Signaling Technology, Beverly, MA); anti-Rb (BD Transduction Laboratories); anti-actin and anti-vinculin (Sigma). Either anti-mouse or anti-rabbit horseradish peroxidase (1:3000, Bio-Rad) were used as secondary antibodies. Bands were visualized by enhanced chemoluminescence.

RT-PCR—Cells were lysed with TRIzol, and total RNA was extracted according to the manufacturer's protocol (Invitrogen). Total RNA (5 μg) from each sample was reverse-transcribed using SuperScript™ II reverse transcriptase (Invitrogen). cDNA (2 μl) was subject to 20 PCR amplification cycles using the following primers: $p21^{Cip1}$ forward 5′-GCGATGGAACTTCGACTTTGT and $p21^{Cip1}$ reverse 5′-GGGCTTCCTCTTGGAGAAGAT; GADPH forward 5′-TGAAGGTCGGAGTCAACGGATTT and GADPH reverse 5′-GATGGGATTTCCATTGATGACAAGC.

RNA Interference (RNAi)—21-bp dsRNAs were purchased from Dharmacon Research, Inc. (Dallas, TX) or Ambion (Austin, TX) and transfected into H358 cells using Oligofectamine (Invitrogen) following the protocol provided by the manufacturer. The following targeting sequences were used: PKCα (1: AATCCTTGTCCAAGGAGGCTG; 2: GAACAACAAGGAATGACTT), $p21^{Cip1}$ (1: AACATACTGGCCTGGACTGTT; 2: ATCGTCCAGCGACCTTCCT), and a control unrelated sequence (Silencer® negative control 7 siRNAi, Ambion).

Plasmid Transfections and Promoter Analyses—H358 cells in 12-well plates (5×10^4 cells/well) were transiently transfected with 0.5 μg of a $p21^{Cip1}$ Firefly luciferase reporter vector (26) using Fugene 6 (Roche Applied Science, Indianapolis, IN). A *Renilla* luciferase expression vector (50 ng, pRL-TK, Promega, Madison, WI) was co-transfected for normalization of transfection efficiency. After transfection, cells were grown overnight in complete medium, synchronized at the G_1/S boundary, and lysed. Cells extracts were subject to luciferase determination using the Dual-Luciferase Reporter Assay System (Promega). Results were expressed as the ratio between Firefly and *Renilla* luciferase.

Immunofluorescence—Cells were plated on coverslides placed on 35-mm dishes. After synchronization, cells were stimulated with either PMA or vehicle, and at the indicated times washed twice with PBS, fixed for 10 min with methanol, washed three times for 5 min with PBS, and permeabilized for 15 min with 0.25% Triton X-100 in PBS, followed by a 10-min incubation in 100 mM glycine in PBS. After blocking for 30 min with 3% fetal bovine serum in PBS, a mouse anti-$p21^{Cip1}$ monoclonal antibody (1:250) was added (1 h), followed by washing with 0.1% Tween-20 in PBS, and incubation with a CY3-conjugated anti-mouse antibody (1:1000; Jackson Immunoresearch Laboratories, Inc.) was added. After additional washings, DNA was stained using DAPI (0.1 μg/ml, 10 min). Coverslides were washed three times with PBS, mounted with Vectashield, and visualized with a Nikon Eclipse TE2000 inverted microscope equipped with a q-imaging Exi digital cooled camera (1360 × 1036 pixels, Burnaby, Canada). Recordings were done using Northern Eclipse 6.0 software (Empix Imaging Inc., Cheektowaga, NY). A 40× planar objective (Nikon) was used for all recordings.

Subcellular Fractionation—Cells were washed, collected in ice-cold PBS, and then pelleted and fractionated into cytosolic and nuclear fractions, as described elsewhere (27). Separation of cytosolic and particulate fractions was performed by ultracentrifugation, as described previously (28).

Determination of Senescence-associated β-Galactosidase Activity—Senescence-associated β-Galactosidase (SA-β-Gal) staining was carried out as described by Dimri *et al.* (29). Briefly, 1×10^5 cells were seeded in 60-mm plates. After synchronization, cells were stimulated with either PMA or vehicle, and 3 days later fixed with 2% formamide/0.2% glutaraldehyde in PBS (10 min, room temperature) and incubated overnight at 37 °C with a solution containing 1 mg/ml 5-bromo-4-chloro-3-indolyl-β-D-galactopyranoside (X-Gal), 5 mM potassium ferrocyanide, 5 mM potassium ferricyanide, 150 mM NaCl, and 2 mM $MgCl_2$ in 40 mM citric acid/sodium phosphate buffer, pH 6.0. 24 h later the percentage of SA-β-Gal-positive (blue) cells in each sample was determined after scoring 300 cells using a bright-field microscope.

Analysis of Telomerase Activity—Non-isotopic telomerase activity was determined by the telomeric repeat amplification protocol (TRAP) using the TRAPEZE® telomerase detection kit (Chemicon International, Temecula, CA) according to the manufacturer's instructions.

Statistical Analysis—Data are presented as mean ± S.D. and were analyzed using a Student's *t* test. A p value of <0.05 was considered statistically significant.

RESULTS

PMA Causes Irreversible G_2/M Arrest in NSCLC Cells—PKC activation with phorbol esters causes a profound inhibition of cell proliferation in lung cancer cells, and our previous work has identified a PKCδ-dependent inhibitory mechanism that limits cell progression from G_1 into S phase (24). However, when asynchronously growing H358 NSCLC cells were treated for 30 min with the PKC activator PMA (100 nM), a significant accumulation of cells in G_2/M was observed, as determined by flow cytometry analysis (Fig. 1*A*, *left panel*). At 48 and 72 h the population of G_2/M cells in response to PMA treatment doubled relative to vehicle-treated cells. A significant accumulation of cells in G_2/M in response to PMA was also observed in H441 and H322 cells (Fig. 1*A*, *right panel*). PKC activation by PMA induces apoptosis in several cellular models (1, 5, 23), but no evidence of apoptosis in response to PMA was observed in H358, H441, or H322 cells either by flow cytometry (absence of a sub-G_0/G_1 cell population) or by microscopy (absence of fragmented nuclei after DAPI staining, data not shown).

To begin dissecting the mechanisms that lead to the accumulation of H358 cells in G_2/M, we decided to synchronize cells with hydroxyurea (HU) and analyze the effects of PMA on S → G_2 progression. Approximately 70% of H358 cells were synchronized in late G_1 after HU treatment. Upon removal of HU by extensive washing, cells began progressing into S phase at ~2 h, and into G_2 phase at ~6 h. HU treatment did not seem to cause significant replicative stress, as judged by the ability of cells to complete the cell cycle (supplemental Fig. S1) and reach confluence, the absence of apoptosis, as well as the possibility of subculturing cells for several passages after HU treatment (data not shown). To analyze the effect of phorbol ester treatment on S → G_2 progression, H358 cells were treated with PMA (100 nM, 30 min) or vehicle 2 h after HU release, and cell cycle distribution was determined at different times. Fig. 1*B* shows that PMA caused a significant delay in S → G_2 transition. Indeed, while it takes 8 h to reach the maximum % of control cells in G_2, this effect is achieved at 11 h in PMA-treated cells. The effect was dependent on the PMA concentration (Fig. 1*C*, *upper panel*), as well as the length of incubation, with maximum response at 30 min (Fig. 1*C*, *center panel*). The S → G_2 delay was observed only when PMA was added in late G_1-early S phase ($t = 2$–5 h) but not when the phorbol ester was added in late S phase ($t = 6$ h) (Fig. 1*C*, *lower panel*). Notably, despite the short duration of the incubation with PMA, the majority of the cells still remained in G_2/M 72 h after treatment (Fig. 1*B*, *right panel*). Therefore, the delay in S → G_2 transition was accompanied by an irreversible arrest that prevented cells to complete

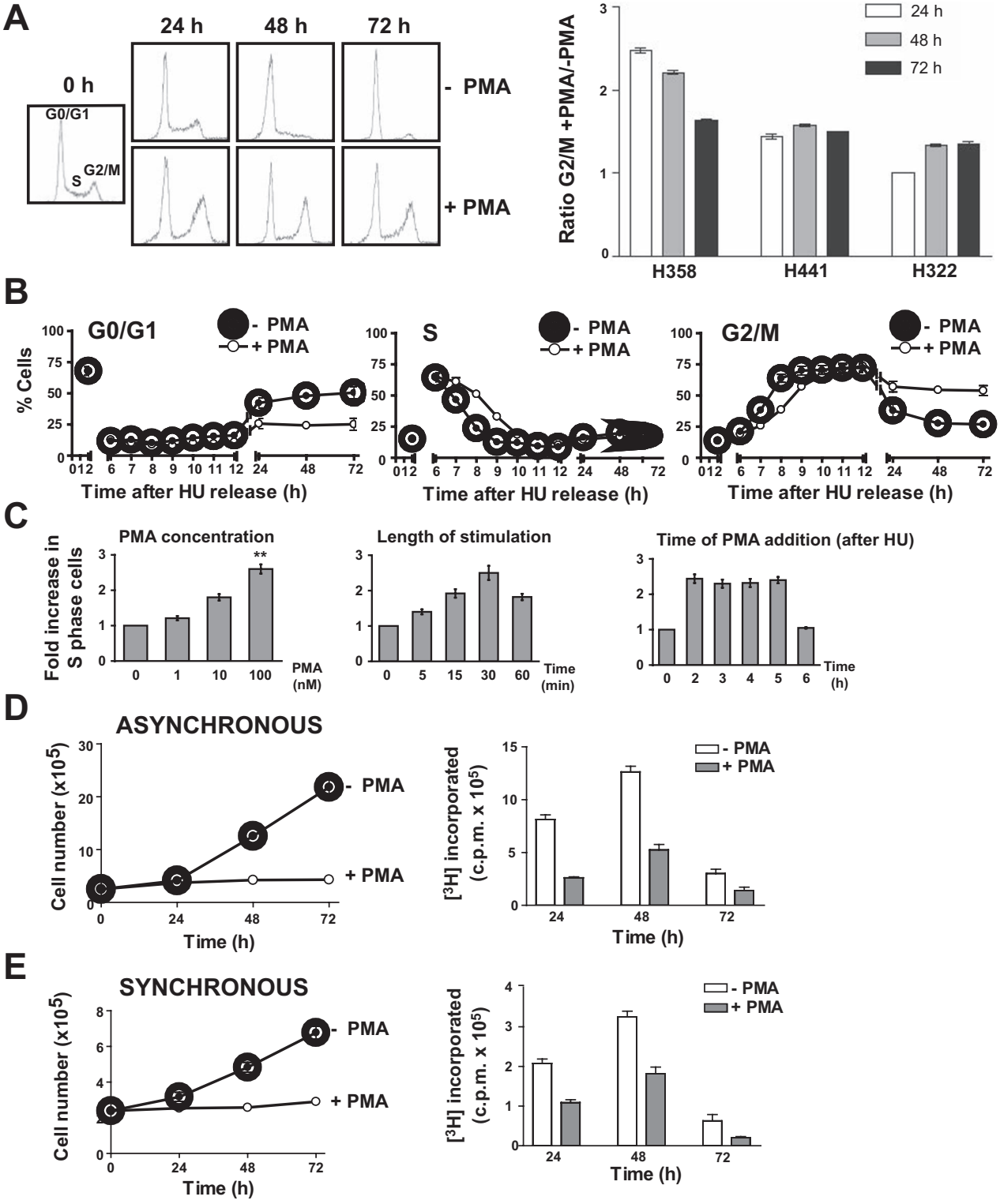

FIGURE 1. **PMA promotes irreversible G_2/M arrest in NSCLC cells.** *A*, asynchronous cultures of cells were treated with 100 nM PMA (+*PMA*) or vehicle (−*PMA*) for 30 min. Cells were collected at 24, 48, or 72 h, stained with propidium iodide and analyzed by flow cytometry. *Left panel*, a representative cell cycle profile for each treatment in H358 cells is shown. *Right panel*, accumulation of H358, H441, and H322 cells in G_2/M in response to PMA; data are presented as mean ± S.D. ($n = 3$), and represent the percentage of increase of cells in G_2/M after PMA treatment relative to vehicle-treated cells. *B*, H358 cells were synchronized in the G_1/S phase boundary with HU, as described under "Experimental Procedures" and released by extensive washing. Cells were treated for 30 min with either vehicle (−*PMA*) or 100 nM PMA (+*PMA*) 2 h after HU release (late G_1-early S, see supplemental Fig. S1*A*). Cells were collected at the indicated times and analyzed for cell cycle distribution using flow cytometry. Results are expressed as mean ± S.D. ($n = 3$). *C*, HU-synchronized H358 cells were stimulated with PMA at different times after HU release and cell cycle distribution was determined at $t = 9$ h (late S-early G_2). *Upper panel*, effect of different PMA concentrations, added at $t = 2$ h for 30 min. *Center panel*, analysis of different lengths of incubation with PMA (100 nM, added at $t = 2$ h). *Low panel*, effect of addition of 100 nM PMA for 30 min at different times after HU release. Results (mean ± S.D., $n = 3$) are expressed as fold-increase in the number of cells in S phase. *D*, cells synchronized with HU were released and treated with PMA (100 nM, 30 min) 2 h after release. *Left panel*, cell number; *right panel*, [^{3}H]thymidine incorporation. *E*, asynchronous H358 cells were treated with PMA (100 nM, 30 min) and cell number (*left panel*) or [^{3}H]thymidine incorporation (*right panel*) were determined. For all panels, two additional experiments gave similar results.

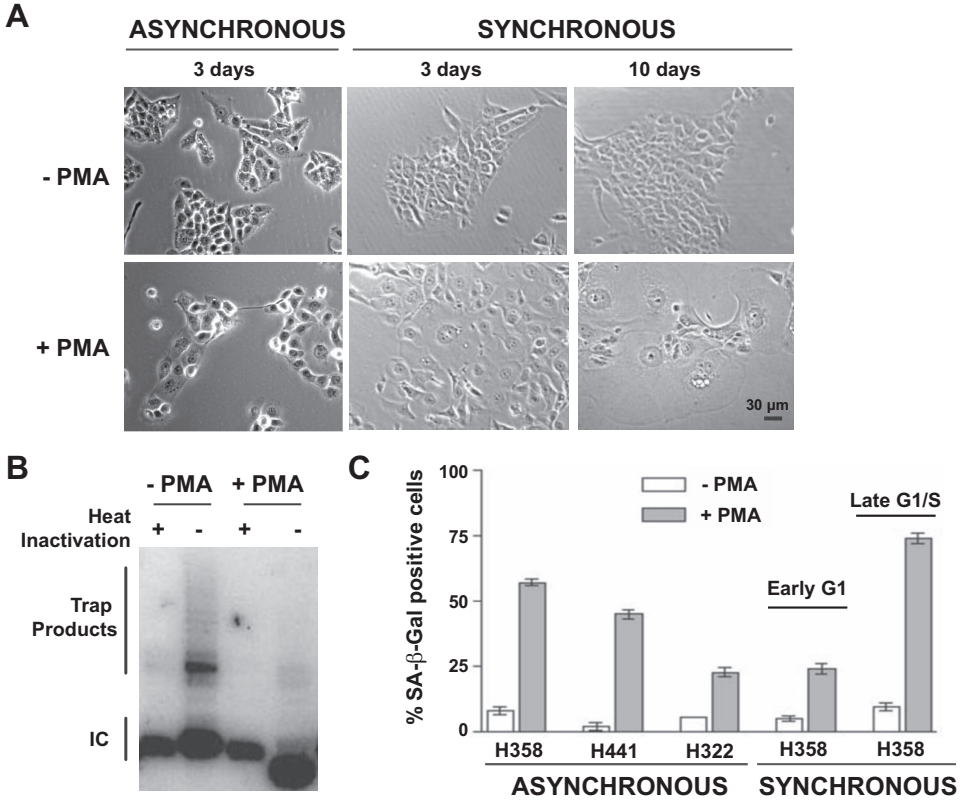

FIGURE 2. **PMA induces senescence in a cell cycle phase-specific manner in NSCLC cells.** *A*, asynchronous or HU-synchronized H358 cells were treated with PMA (100 nM, 30 min, 2 h after HU release for the synchronized cells), and cell morphology was recorded by phase-contrast micrograph 3 and 10 days after treatment. *B*, HU-synchronized H358 cells were treated with PMA (100 nM, 30 min, added at $t = 2$ h), and 3 days later telomerase activity was assayed by TRAP, as described under "Experimental Procedures." Three experiments gave similar results. Inactivation by heat of telomerase from cell lysates was included as a negative control. *IC*, internal control for PCR efficiency. *C*, induction of SA-β-Gal activity was assessed 3 days after PMA treatment (100 nM, 30 min). Treatment was carried out in asynchronous cultures, 2 h after HU release (*late* G_1/*S*), or after addition of serum to cells arrested in G_0 by 24 h serum starvation (*early* G_1), as in Nakagawa *et al.* (24). Data are expressed as mean ± S.E. ($n = 4–6$).

the cycle and progress into G_1. Indeed, treatment of cells synchronized in the G_1/S phase boundary ($t = 2$ h after HU release) with 100 nM PMA (30 min) abolished proliferation, as determined by cell counting (Fig. 1*D*, *left panel*). In agreement with this data, PMA treatment of HU-synchronized cells resulted in a marked inhibition of DNA synthesis, as judged by analysis of [^{3}H]thymidine incorporation (Fig. 1*D*, *right panel*). Irreversible arrest by PMA was also observed in asynchronous cultures of H358 cells, as determined both by cell counting and [^{3}H]thymidine incorporation (Fig. 1*E*). Thus, PMA treatment of H358 cells in S phase leads to irreversible accumulation of cells in G_2, arguing for multiple points of regulation of the cell cycle by PKC activation.

PMA Induces Senescence in H358 Cells in a Cell Cycle Phase-specific Manner—Morphological analysis of H358, H441, and H322 cells 72 h after PMA treatment, either in asynchronous or HU-synchronized cultures, showed that a significant number of cells became large and flat, and exhibited enlarged nuclei. These features, together with irreversible growth, are hallmarks of senescence (30). Remarkably, cells remain attached for at least 10 days post-PMA treatment. At that time the phenotypic changes were more pronounced (Fig. 2*A*), with cells even larger, multinucleated, and with a characteristic vacuolization. We then determined the effect of PMA on telomerase activity, using a telomeric repeat amplification protocol (TRAP). PMA treatment in S phase caused a significant reduction of telomerase activity in H358 cells (Fig. 2*B*). To further establish the presence of a senescence phenotype, we measured the expression of SA-β-Gal, a well-established marker of senescence (29). Notably, >50% of H358 cells in asynchronous cultures became SA-β-Gal positive after PMA treatment, compared with <10% in response to vehicle. Similarly, a significant fraction of H441 and H322 become SA-β-Gal positive (Fig. 2*C*). The proportion of SA-β-Gal positive H358 cells was even higher (>75%) when PMA treatment was carried out in HU-synchronized cells. However, when PMA was added to H358 cells synchronized in early G_1 phase, there was only a slight increase in the number of β-Gal positive cells. Therefore, the PMA effect is phase specific, as senescence does not occur when PKC activation was triggered in early G_1. Altogether, these data strongly suggest that the irreversible G_2/M arrest induced by PMA during S phase leads to senescence. The senescence phenotype was also observed in H460 lung cancer cells, as well as in HT-29 and HCT-116 colon cancer cells.[5]

$p21^{Cip1}$ Is Required for PMA-induced G_2/M Arrest and Senescence Induction—Analysis of relevant cell cycle markers in NSCLC cells upon HU release revealed a marked elevation in the levels of the Cdk inhibitor $p21^{Cip1}$ in response to PMA, which was sustained even 72 h after treatment (Fig. 3, *A* and *B*). $p21^{Cip1}$ up-regulation is a characteristic feature of senescent cells (31). Additional studies in H358 cells revealed no significant changes in p27 levels. PMA treatment led to a marked reduction in Rb phosphorylation and in the levels of the transcription factor E2F-1. A sustained reduction in the levels of cyclin E, cyclin A, and cyclin B, as well as induction of cyclin D1, were also observed (Fig. 3*B*). While the levels of $p21^{Cip1}$ protein did not change significantly across S phase in H358 cells after HU release (Fig. 3*C*, *upper panel*, *−PMA*), a progressive $p21^{Cip1}$ up-regulation was observed in response to PMA (Fig. 3*C*, *upper panel*, *+PMA*). Similar results were observed at the mRNA level, as determined by RT-PCR (Fig. 3*C*, *lower panel*). In addition, PMA treatment of HU-synchronized cells promoted a sig-

[5] M. C. Caino, J. L. Oliva, and M. G. Kazanietz, data not shown.

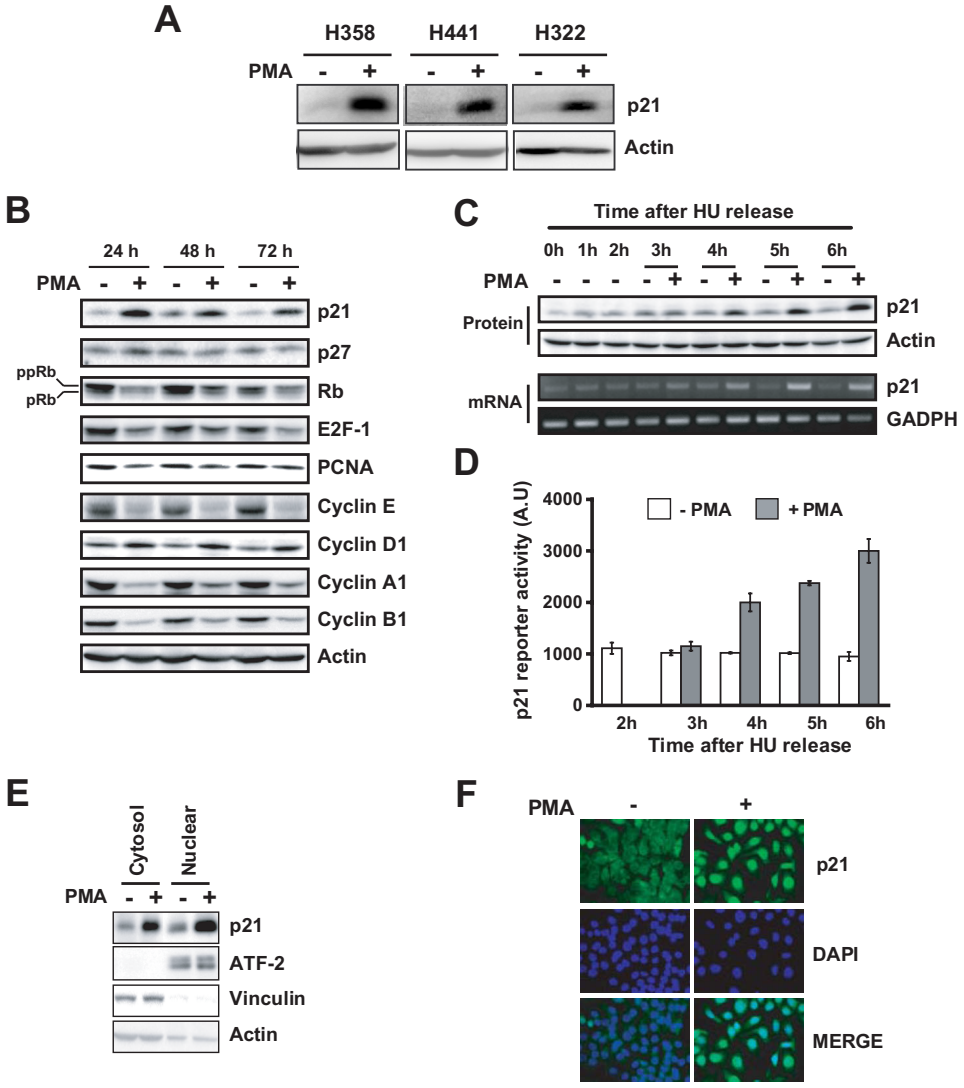

FIGURE 3. **PMA up-regulates p21^{Cip1} during S phase in NSCLC cells.** HU-synchronized H358, H441, or H322 cells were treated with PMA (100 nM, 30 min) or vehicle, 2 h after HU release ($t = 2$ h). All experiments were carried out three times with similar results. *A*, Western blot of p21^{Cip1} 4 h after PMA treatment ($t = 6$ h post-release). *B*, Western blot analysis of relevant cell cycle markers 24, 48, or 72 h after treatment in H358 cells. *C*, analysis of p21^{Cip1} protein (*upper panel*) and mRNA (*lower panel*) levels from 0–6 h after HU release in H358 cells. *D*, H358 cells were co-transfected with a p21^{Cip1} Firefly luciferase reporter and pTK-*Renilla* 24 h prior to synchronization with HU. Firefly luciferase activity was determined at the indicated times after HU release and normalized to *Renilla* luciferase activity. Results, as arbitrary units (*A.U.*) are expressed as mean ± S.D. ($n = 3$). *E*, H358 cell extracts were collected 4 h after PMA treatment ($t = 6$ h after HU release) and subject to fractionation as described under "Experimental Procedures." p21^{Cip1} protein was determined by Western blot in cytosolic and nuclear fractions. ATF-2 and vinculin were used as markers for the nuclear and cytosolic fractions, respectively. *F*, localization of p21^{Cip1} by immunofluorescence in H358 cells 4 h after PMA treatment ($t = 6$ h). *Green*, p21^{Cip1}; *blue*, DAPI.

nificant activation of a p21^{Cip1} luciferase reporter (Fig. 3*D*). As newly synthesized p21^{Cip1} protein translocates to the nucleus to exert its inhibitory activity on cyclin-Cdk complexes (32), we carried out a subcellular fractionation analysis. ATF-2 and vinculin were used as controls for the nuclear and cytosolic fractions, respectively. A marked elevation of nuclear p21^{Cip1} in response to PMA was observed (Fig. 3*E*). Elevated p21^{Cip1} levels were also detected in the cytosolic fraction, which probably reflects protein recently synthesized. Likewise, immunofluorescence staining revealed a prominent nuclear p21^{Cip1} staining in PMA-treated compared with vehicle-treated H358 cells (Fig. 3*F*).

To determine whether a causal relationship exists between p21^{Cip1} up-regulation, G_2/M arrest and the senescent phenotype, we used a RNAi approach. Two different RNAi target sequences were used in order to minimize the chances of off-target effects. H358 cells were transfected with either p21^{Cip1} RNAi or control duplexes, and 24 h later cells were HU-synchronized and treated with either PMA or vehicle. A >90% reduction in the induction of p21^{Cip1} was achieved with either RNAi duplex (Fig. 4*A*), which lasted for at least 4 days (data not shown). p21^{Cip1} depletion did not affect the synchronization protocol (supplemental Fig. S2). Notably, p21^{Cip1}-depleted H358 cells failed to arrest in G_2/M in response to PMA (Fig. 4*B*). Moreover, p21^{Cip1} RNAi markedly reduced the induction of the senescence marker SA-β-Gal by the phorbol ester (Fig. 4*C*). Therefore, p21^{Cip1} up-regulation is required for G_2/M arrest and the induction of a senescence phenotype by PMA in H358 cells.

PMA-induced p21^{Cip1} Up-regulation, G_2/M Arrest, and Senescence Are Mediated by PKCα—H358, H441, and H322 cells express three phorbol ester-responsive PKCs: the classical PKCα, and the novel PKCs δ and ε (24, and data not shown). While PKCε is mostly a mitogenic/survival kinase, growth inhibitory roles have been ascribed to PKCα and/or PKCδ in several cell models. We have previously described that PKCδ mediates PMA-induced G_1 arrest in H358 cells (24). Expression levels of PKCα, PKCδ, and PKCε in H358 cells remained constant across the S phase (supplemental Fig. S3*A*). To determine the involvement of PKC isozymes in p21^{Cip1} induction by PMA we first used a pharmacological approach. As we have found that translocation of PKCα, PKCδ, and PKCε in response to PMA (a hallmark of PKC activation) remained for the whole S phase (Fig. S3*B*), PKC inhibitors were added before PMA treatment (−50 min) and left until the end of the S phase. As shown in Fig. 5*A*, the pan-PKC inhibitor GF109203X (bisindolylmaleimide I) completely blocked p21^{Cip1} up-regulation by PMA in H358, H441, and H322 cells. Gö6976, a specific inhibitor of cPKCs (33), also blocked p21^{Cip1} up-regulation. On the other hand, the PKCδ inhibitor rottlerin was ineffective or less effective. As PKCα is the only cPKC pres-

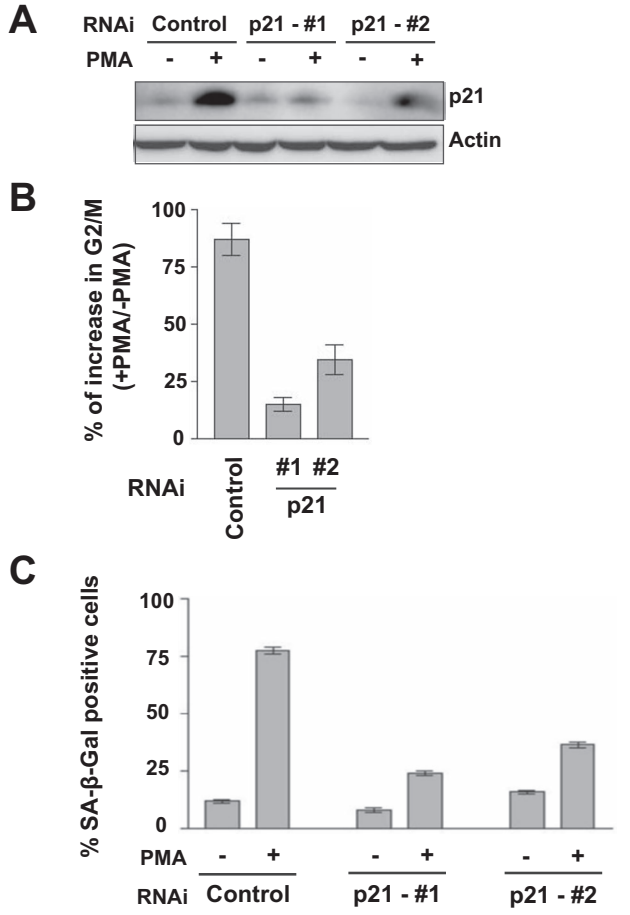

FIGURE 4. **p21^{Cip1} is required for PMA-induced G_2/M arrest and senescence in H358 cells.** H358 cells were transfected with two different p21^{Cip1} duplexes (nos. 1 or 2) or a control RNAi duplex, 24 h before HU-synchronization, and then treated with PMA (100 nM, 30 min, $t = 2$ h after HU release). *A*, expression of p21^{cip1}, 4 h after PMA treatment ($t = 6$ h after HU release). *B*, accumulation of cells in G_2/M in response to PMA; data are presented as mean ± S.D. ($n = 3$), and represent the percentage of increase of cells in G_2/M after PMA treatment relative to vehicle-treated cells. Similar results were observed in four independent experiments. *C*, determination of SA-β-Gal activity 72 h after PMA treatment. Data are expressed as mean ± S.D. Three additional experiments gave similar results.

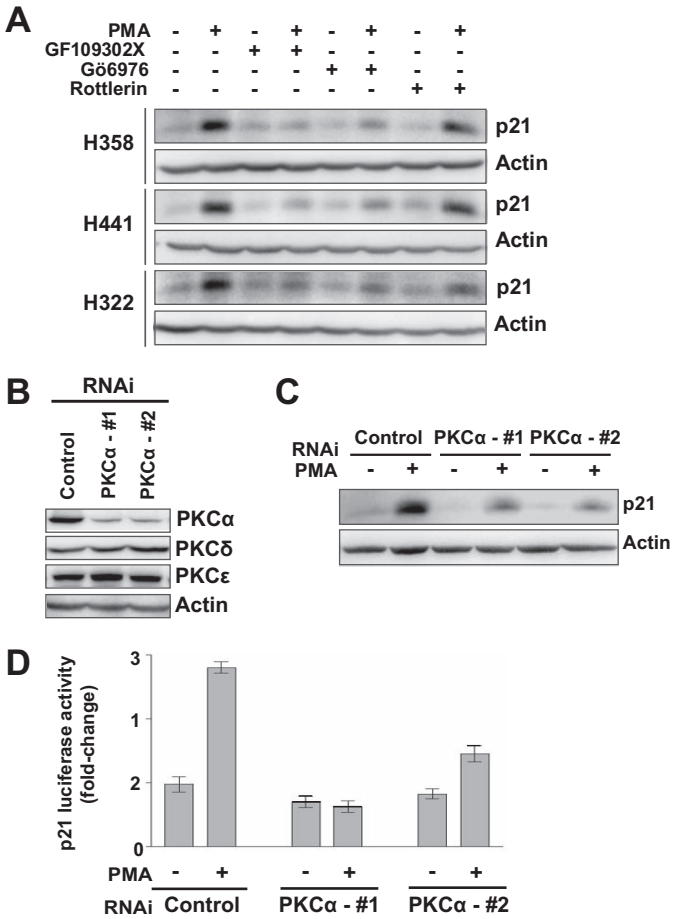

FIGURE 5. **PKCα mediates PMA-induced p21^{Cip1} up-regulation in NSCLC cells.** *A*, PKC inhibitors (5 μM) were added 50 min before PMA treatment (100 nM, 30 min, $t = 2$ h) and left in the medium until $t = 6$ h. At that time, cell lysates were prepared and subject to Western blot analysis. A representative blot of three independent experiments is shown. *B–D*, H358 cells were transfected with two different PKCα duplexes (nos. 1 or 2) or a control RNAi duplex, 24 h before HU-synchronization, and analyzed for PKC isozyme expression (*B*), or then treated with PMA (100 nM, 30 min, $t = 2$ h after HU release) and subject to Western blot for p21^{Cip1} (*C*) or luciferase reporter analysis (*D*) at $t = 6$ h. For the luciferase studies, 24 h after transfection with RNAi duplexes, cells were co-transfected with a p21^{Cip1} Firefly luciferase reporter and pTK-*Renilla*. Results represent the ratio between Firefly and *Renilla* luciferase activity, and are expressed as fold-induction relative to vehicle-treated cells transfected with the control RNAi duplex. Data are expressed as mean ± S.D. ($n = 3$). Four experiments gave similar results.

ent in H358 cells, these experiments suggest that this PKC mediates p21^{Cip1} induction, and presumably also mediates G_2/M arrest. To determine the involvement of PKCα in mediating the G_2/M arrest we used RNAi. Fig. 5*B* shows that >90% reduction in PKCα levels was achieved upon delivery of two different specific PKCα RNAi duplexes into H358 cells, without affecting the expression of other phorbol ester-responsive PKC isozymes (Fig. 5*B*). In agreement with the results using inhibitors, PKCα depletion impaired PMA-induced up-regulation of p21^{Cip1} (Fig. 5*C*), suggesting a crucial role for this cPKC in mediating p21^{Cip1} up-regulation in S phase. Moreover, in PKCα-depleted cells PMA failed to stimulate p21^{Cip1} reporter luciferase activity (Fig. 5*D*).

Because p21^{Cip1} up-regulation is required for G_2/M arrest and senescence induced by PMA, we reasoned that PKCα is involved in mediating the senescence phenotype. Analysis of cell cycle distribution revealed that PKCα-depletion impaired PMA-induced G_2/M arrest in H358 cells (Fig. 6*A*). Interestingly, in PKCα-depleted cells the morphological alterations induced by PMA could not be observed (Fig. 6*B*). Moreover, the percentage of SA-β-Gal-positive cells as a consequence of PMA stimulation was drastically reduced in H358 cells subject to PKCα RNAi (Fig. 6*C*). Furthermore, when PKCα was knocked down, the inhibitory effect of PMA on telomerase activity was impaired (Fig. 6*D*).

In the last set of experiments we used an adenoviral approach to overexpress PKCα. H358 cells were infected with either control LacZ or PKCα AdVs (24). Cells were synchronized with HU and subject to PMA treatment, as described above. Neither LacZ nor PKCα overexpression affected the synchronization protocol (supplemental Fig. S4). Interestingly, the induction of p21^{Cip1} expression by PMA was significantly enhanced in PKCα-overexpressing H358 cells (Fig. 7*A*). While overexpression of PKCα using 100 MOI of PKCα AdV did not cause significant p21^{Cip1} up-regulation in the absence of PMA stimula-

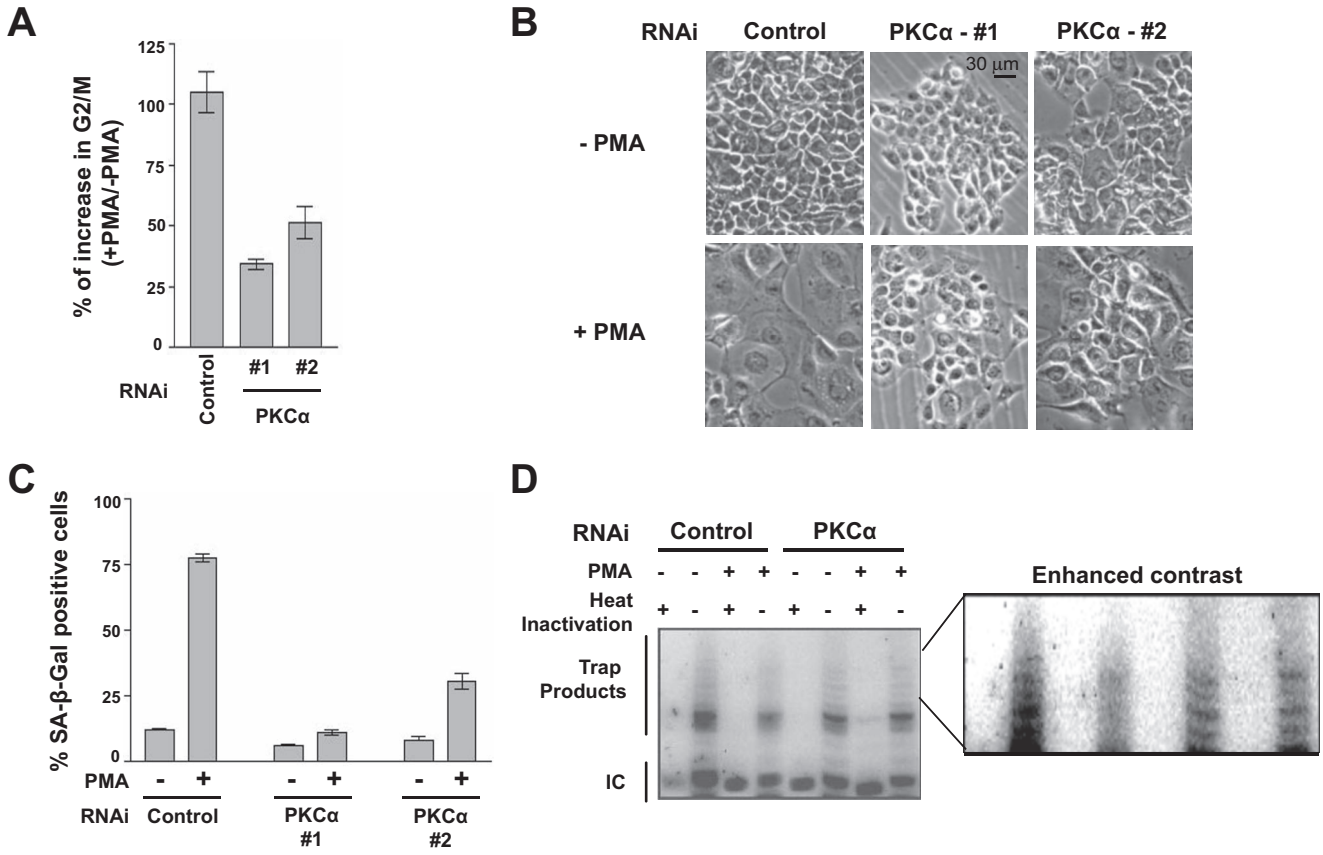

FIGURE 6. **PKCα RNAi impairs both PMA-induced G_2/M arrest and senescence of H358 cells.** Cells were transfected with two different PKCα duplexes (nos. 1 or 2) or a control RNAi duplex. 24 h later cells were synchronized with HU and treated with PMA (100 nM, 30 min) or vehicle 2 h after HU release. *A*, accumulation of cells in G_2/M in response to PMA; data are presented as mean ± S.D. ($n = 3$), and represent the percentage of increase of cells in G_2/M after PMA treatment relative to vehicle-treated cells. *B*, cell morphology, as determined by phase-contrast microscopy 72 h after PMA (+*PMA*) or vehicle (−*PMA*) treatment. *C*, determination of SA-β-Gal activity 72 h after PMA treatment. Results are expressed as mean ± S.D. ($n = 3$). *D*, determination of telomerase activity 72 h after PMA treatment using the TRAP assay, as described under "Experimental Procedures." Inactivation by heat of telomerase from cell lysates was included as a negative control. *IC*, internal control for PCR efficiency in the TRAP assay. In all cases, at least three independent experiments were carried out, and similar results were obtained.

tion, higher MOIs (500 pfu/cell) slightly increase the basal levels of $p21^{Cip1}$ (data not shown). The percentage of cells accumulated in G2/M in response to PMA was higher in PKCα AdV-infected cells (100 MOI) compared with control cells (Fig. 7*B*). Lastly, we took advantage of a specific PKCα agonist, the DAG-lactone HK-434 (34). Treatment of H358 cells with HK-434 induced $p21^{Cip1}$ levels to a similar extent than PMA (Fig. 7*C*). Furthermore, HK-434 caused a marked accumulation of cells in G_2/M (Fig. 7*D*), as well as characteristic senescence features, including cell flattening and enlargement (Fig. 7*E*), and induction of SA-β-Gal activity (Fig. 7*F*). Taken together, these data strongly suggest that activation of PKCα by PMA during S phase leads to $p21^{Cip1}$ up-regulation, irreversible G_2/M arrest, and the induction of a senescence phenotype in H358 lung cancer cells.

DISCUSSION

A considerable body of evidence supports the notion that the differential proliferative *versus* antiproliferative effects of phorbol esters is conferred by the distinct ability of PKC isozymes to regulate the cell cycle machinery. This study introduces three novel paradigms. The first is that activation of PKCα can lead to a senescence phenotype, an effect mediated by the induction of $p21^{Cip1}$. Second, senescence is strictly dependent upon the phase of the cell cycle in which PKC activation occurs. Third, this is the first study to our knowledge showing that in a defined cellular model phorbol esters trigger cell arrest in different phases of the cell cycle via a common mechanism ($p21^{Cip1}$ induction) but through distinct PKC isozymes. Our previous studies have shown that phorbol ester treatment of lung cancer cells in early G_1 impairs their progression into S phase. This G_1 arrest is mediated by PKCδ (24). In contrast, when cells are treated with PMA in late G_1 or S phases, they undergo permanent arrest in G_2/M accompanied by senescence, and in this case the effect is mediated by PKCα rather than PKCδ. Despite the differential involvement of PKC isozymes, both effects occur via the up-regulation of the cell cycle inhibitor $p21^{Cip1}$. These cell cycle phase-specific effects not only attest to the functional complexity of PKC isozymes, but also suggest that PKC regulation of cell cycle via $p21^{Cip1}$ involves multiple mechanisms.

While phorbol esters are mitogenic in some cellular models (35, 36), they can also inhibit proliferation or promote apoptosis in a large number of cell types. Dual G_0/G_1 and G_2/M arrest by phorbol esters has been reported in endothelial (13), breast cancer (37) and melanoma cells (38). PKCα was shown to play

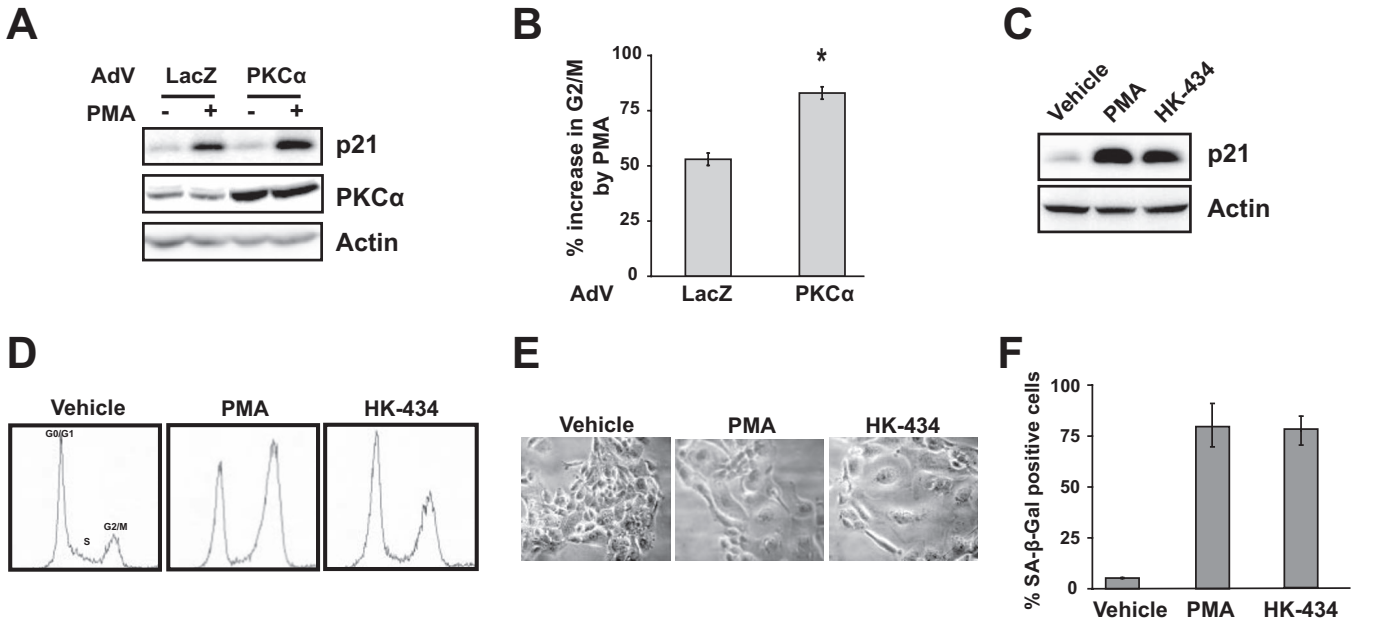

FIGURE 7. **PKCα selective activation during S phase induces $p21^{Cip1}$ up-regulation, G_2/M arrest and senescence.** *A* and *B*, H358 cells were infected with either PKCα or LacZ (control) AdVs (MOI = 100 pfu/cell) and 24 h later synchronized with HU. 2 h after HU release, cells were treated with PMA (100 nM, 30 min). 24 h after PMA treatment, cells were subject to Western blot (*A*) or flow cytometry analysis (*B*). Data are expressed as mean ± S.D. ($n = 3$). *, $p < 0.05$. Three additional experiments gave similar results. *C–F*, HU-synchronized H358 cells were stimulated with the DAG-lactone HK-434 (10 μM, 30 min), PMA (100 nM, 30 min), or vehicle, 2 h after HU release. *C*, $p21^{Cip1}$ expression was assessed by Western blot at $t = 6$ h. *D*, cell cycle analysis was performed 24 h after treatment. *E*, cell morphology 3 days after treatment. *F*, determination of SA-β-Gal activity 3 days after treatment; data are expressed as mean ± S.D. Three additional experiments gave similar results.

negatives roles in $G_1 \rightarrow S$ transition as well as in $G_2 \rightarrow M$ transition (4, 5, 38, 39). However, there has been little information on the role of PKC activation in S phase. It has been reported that in G_1/S-synchronized Demel and MCF-7 cells, phorbol ester stimulation induces a transitory G_2 arrest (37, 38). This fits well with our observations that in H358 lung cancer cells PKC activation in late G_1 or early S phases causes a significant delay in $S \rightarrow G_2$ transition. In addition to this effect, our data provide strong evidence that PMA activation promotes irreversible G_2/M arrest and inhibition of proliferation by inducing cellular senescence. The cellular senescent phenotype is defined by the appearance of characteristic morphological changes and biochemical markers, including the induction of SA-β-Gal activity and $p21^{cip1}$, and inhibition of telomerase activity, leading ultimately to irreversible proliferation arrest. Cellular senescence has been originally described in primary cells as a consequence of telomere shortening (40). However, senescence can be also triggered by a variety of signals such as DNA damage, loss of tumor suppressors, and oncogenic hyperproliferative signals (30). The fact that PMA triggers cellular senescence in lung cancer cells argues for the existence of senescence mechanisms dependent on PKC. In support of our data, a very recent study has shown that long-term (24 h) treatment with the diterpene ester PEP005 induces irreversible cell cycle arrest in G_1 and G_2/M phases and senescence in melanoma cells via PKC (41). However, long-term PKC activation leads to PKC down-regulation, and therefore it is unclear from that study whether PKC activation or PKC depletion was responsible for the phenotype in melanoma cells, as well as which PKC isozymes were responsible for the effect. In our studies in H358 cells, a short incubation with PMA is capable of inducing senescence, suggesting that PKCα activation rather than down-regulation is triggering a senescence program. Indeed, we do not detect PKC down-regulation as a consequence of the PMA treatment (supplemental Fig. S3*B*). Interestingly, H358 lung cancer cells go into senescence when treated with PMA in late G_1-S, but only a small percentage of cells undergo a senescence phenotype when treated with PMA in early G_1. This small fraction of senescent cells may arise from cells in late G_1 present as a consequence of incomplete G_0 synchronization by serum starvation (24). Altogether, these results argue that the senescent population originates from cells arrested in G_2/M.

Although the molecular mechanisms underlying the induction of senescence by PKCα still require investigation, our studies unambiguously show the involvement of the cell cycle inhibitor $p21^{Cip1}$. PMA promotes a robust elevation in $p21^{Cip1}$ mRNA and protein levels during S phase. Furthermore, $p21^{Cip1}$ up-regulation represents an obligated event, as $p21^{Cip1}$ RNAi significantly impaired the induction of G_2/M arrest and senescence by the phorbol ester. PKCα RNAi depletion inhibited the induction of $p21^{Cip1}$ by PMA, both at the level of mRNA (data not shown) and protein, and consequently blocked the induction of G_2/M arrest and senescence by PMA, thus providing strong evidence for a PKCα-$p21^{Cip1}$-G_2 arrest-senescence link. The unique phenotypes observed in response to PKC activation at different cell cycle phases probably reflect distinct roles for $p21^{Cip1}$ in G_1 and G_2. Indeed, while $p21^{Cip1}$ is an inhibitor of G_1 cyclin-Cdk complexes, it also inhibits the activation of Cdc2 in G_2 (42, 43). PKCα was shown to play a role in G_1/S arrest via p21 induction and to mediate cell cycle exit and a differentiation program in intestinal cells (4), suggesting that this cPKC can

exert multiple effects depending on the cell type. $p21^{Cip1}$ mRNA stability can be regulated by diverse factors such as the RNA-binding proteins HuR and CP1 (44). A very recent study showed that PKCα modulates HuR nuclear-cytosolic shuttling, thus favoring mRNA stabilization (45). One attractive hypothesis is that the specific PKCα-mediated $p21^{Cip1}$ up-regulation in late G_1/S phase could be mediated by HuR-dependent $p21^{Cip1}$ mRNA stabilization. However, preliminary studies have not revealed any noticeable changes in HuR total levels or relocalization during G_1, S, or G_2, either in response to PMA treatment or after PKCα overexpression (data not shown). Further studies would be required to address the mechanistic basis of the differential regulation of $p21^{Cip1}$ by PKCs.

Which of the major senescence pathway(s) play a role in PMA-induced senescence? Most senescence responses converge on either p53 (involving DNA damage) and/or pRB (mostly through stress or oncogene activation of p16) (30). It is well established that DNA lesions can trigger a checkpoint, which delays cell cycle progression and activate DNA-repair mechanisms (reviewed in Ref. 46). Preliminary data show no detectable Chk-1 or histone H2A.X phosphorylation during S-phase in response to PMA (data not shown), suggesting the absence of checkpoint activation by PKCα. It has been postulated that G_2 arrest via $p21^{Cip1}$ induction may involve the suppression of cdk2/cyclin A and cdc2/cyclin B activities, changes in cdc2 phosphorylation status, and inhibition of cdc25 expression (4). PKC activation can inhibit Cdc2 and entry into mitosis by reducing the activity of Cdc25 phosphatases (which dephosphorylate and activate Cdc2), a mechanism that bypasses Chk1 (38). H358 cells do not express p16 (47), suggesting that senescence is independent of this cell cycle inhibitor. Also, the cell lines used in this study are p53-null or mutant (48, 49), arguing for a p53-independent mechanism in the induction of $p21^{Cip1}$ by PKCα. Recent studies have implicated ERK activation as a mediator of p53-independent $p21^{Cip1}$ induction and G_2/M arrest in response to PMA (50). $p21^{Cip1}$ up-regulation in HeLa and SKOV-3 cells in response to growth factors, oxidative stress, or PMA is dependent upon the ERK MAPK cascade (10, 51, 52). Regulation of $p21^{Cip1}$ via ERK may involve transcriptional or post-transcriptional mechanisms that extend $p21^{Cip1}$ half-life (26, 53). Pharmacological inhibition of MEK blocks the senescence phenotype triggered by the diterpene PEP005 in melanoma cells (41). We have observed a strong and sustained activation of ERK in H358 cells upon PMA stimulation that preceded $p21^{Cip1}$ up-regulation in S phase, and we found that MEK inhibition markedly reduced $p21^{Cip1}$ mRNA and protein up-regulation (data not shown), suggesting that a similar mechanism might take place in lung cancer cells.

NSCLC cells are very resistant to conventional anti-cancer treatment. Induction of cellular senescence has been proposed as a strategy for cancer therapy (reviewed in Ref. 54). Studies in breast cancer have shown that induction of senescence following adjuvant therapy correlates with favorable outcome (55). One attractive scenario is that targeting PKCα in NSCLC with specific activators may promote senescence in tumor cells. Our studies strongly suggest that activation rather than inhibition of PKCα function/expression may serve for therapeutic purposes, and may help to explain the failure of PKCα antisense approaches for NSCLC treatment (20). Indeed, PKC agonists have been examined as antitumor agents *in vivo*. Bryostatin 1, a potent PKC activator that induces only a subset of those responses induced by PMA, has been in clinical trials for a number of malignancies, including lung cancer (1, 17). Moreover, PMA has been administered to patients for the treatment of hematological malignancies (15–17). DAG lactones that selectively activate PKCα have anti-proliferative activity not only in lung cancer cells but also in other cancer cell lines (34). The fact that senescence induction in normal cells may facilitate tumor progression (56) argues for the need of additional studies to better assess the validity of PKCα or downstream effectors as a therapeutic targets.

In summary, our studies established that activation of PKCα in lung cancer cells during late G_1-early S phase leads to cellular senescence, an effect that involves $p21^{Cip1}$ up-regulation and irreversible inhibition of cell proliferation. In addition, our results revealed important differences with regards to the role of individual PKC isozymes in different phases of the cell cycle. In our previous study we demonstrated that PMA-induced activation of PKCδ in early-mid G_1 inhibits H358 cell progression into S phase, inducing cell accumulation in G_1 (24), whereas PKCα was dispensable for this effect. The unique growth inhibitory effect of PKC isozymes in specific phases of the cell cycle opens a window of opportunity for targeting individual PKCs for therapeutic purposes.

Acknowledgments—We thank Dr. Victor E. Marquez (Center for Cancer Research, NCI-Frederick), for providing the DAG-lactone HK-434 and Dr. Steven Albelda (University of Pennsylvania) for providing H322 cells.

REFERENCES

1. Griner, E. M., and Kazanietz, M. G. (2007) *Nat. Rev. Cancer* **7,** 281–294
2. Newton, A. C. (2001) *Chem. Rev.* **101,** 2353–2364
3. Fishman, D. D., Segal, S., and Livneh, E. (1998) *Int. J. Oncol.* **12,** 181–186
4. Black, J. D. (2000) *Front Biosci.* **5,** D406–D423
5. Gavrielides, M. V., Frijhoff, A. F., Conti, C. J., and Kazanietz, M. G. (2004) *Curr. Drug Targets* **5,** 431–443
6. Zhou, W., Takuwa, N., Kumada, M., and Takuwa, Y. (1993) *J. Biol. Chem.* **268,** 23041–23048
7. Soh, J. W., and Weinstein, I. B. (2003) *J. Biol. Chem.* **278,** 34709–34716
8. Ohba, M., Ishino, K., Kashiwagi, M., Kawabe, S., Chida, K., Huh, N. H., and Kuroki, T. (1998) *Mol. Cell. Biol.* **18,** 5199–5207
9. Kashiwagi, M., Ohba, M., Watanabe, H., Ishino, K., Kasahara, K., Sanai, Y., Taya, Y., and Kuroki, T. (2000) *Oncogene* **19,** 6334–6341
10. Akashi, M., Osawa, Y., Koeffler, H. P., and Hachiya, M. (1999) *Biochem. J.* **337,** 607–616
11. Zeng, Y. X., and el-Deiry, W. S. (1996) *Oncogene* **12,** 1557–1564
12. Thompson, L. J., and Fields, A. P. (1996) *J. Biol. Chem.* **271,** 15045–15053
13. Kosaka, C., Sasaguri, T., Ishida, A., and Ogata, J. (1996) *Am. J. Physiol.* **270,** C170–C178
14. Mackay, H. J., and Twelves, C. J. (2007) *Nat. Rev. Cancer* **7,** 554–562
15. Strair, R. K., Schaar, D., Goodell, L., Aisner, J., Chin, K. V., Eid, J., Senzon, R., Cui, X. X., Han, Z. T., Knox, B., Rabson, A. B., Chang, R., and Conney, A. (2002) *Clin. Cancer Res.* **8,** 2512–2518
16. Han, Z. T., Tong, Y. K., He, L. M., Zhang, Y., Sun, J. Z., Wang, T. Y., Zhang, H., Cui, Y. L., Newmark, H. L., Conney, A. H., and Chang, R. L. (1998) *Proc. Natl. Acad. Sci. U. S. A.* **95,** 5362–5365
17. Barry, O. P., and Kazanietz, M. G. (2001) *Curr. Pharm. Des.* **7,** 1725–1744
18. Schiller, J. H. (2001) *Oncology* **61,** Suppl. 1, 3–13

19. Fong, K. M., Sekido, Y., Gazdar, A. F., and Minna, J. D. (2003) *Thorax* **58,** 892–900
20. Paz-Ares, L., Douillard, J. Y., Koralewski, P., Manegold, C., Smit, E. F., Reyes, J. M., Chang, G. C., John, W. J., Peterson, P. M., Obasaju, C. K., Lahn, M., and Gandara, D. R. (2006) *J. Clin. Oncol.* **24,** 1428–1434
21. Wen-Sheng, W. (2006) *Cancer Lett.* **239,** 27–35
22. Russo, M., Palumbo, R., Mupo, A., Tosto, M., Iacomino, G., Scognamiglio, A., Tedesco, I., Galano, G., and Russo, G. L. (2003) *Oncogene* **22,** 3330–3342
23. Garcia-Bermejo, M. L., Leskow, F. C., Fujii, T., Wang, Q., Blumberg, P. M., Ohba, M., Kuroki, T., Han, K. C., Lee, J., Marquez, V. E., and Kazanietz, M. G. (2002) *J. Biol. Chem.* **277,** 645–655
24. Nakagawa, M., Oliva, J. L., Kothapalli, D., Fournier, A., Assoian, R. K., and Kazanietz, M. G. (2005) *J. Biol. Chem.* **280,** 33926–33934
25. Fujii, T., Garcia-Bermejo, M. L., Bernabo, J. L., Caamano, J., Ohba, M., Kuroki, T., Li, L., Yuspa, S. H., and Kazanietz, M. G. (2000) *J. Biol. Chem.* **275,** 7574–7582
26. Facchinetti, M. M., De Siervi, A., Toskos, D., and Senderowicz, A. M. (2004) *Cancer Res.* **64,** 3629–3637
27. Zhou, B. P., Liao, Y., Xia, W., Spohn, B., Lee, M. H., and Hung, M. C. (2001) *Nat. Cell Biol.* **3,** 245–252
28. Caloca, M. J., Fernandez, N., Lewin, N. E., Ching, D., Modali, R., Blumberg, P. M., and Kazanietz, M. G. (1997) *J. Biol. Chem.* **272,** 26488–26496
29. Dimri, G. P., Lee, X., Basile, G., Acosta, M., Scott, G., Roskelley, C., Medrano, E. E., Linskens, M., Rubelj, I., Pereira-Smith, O., Peacocke, M., and Campisi, J. (1995) *Proc. Natl. Acad. Sci. U. S. A.* **92,** 9363–9367
30. Campisi, J. (2005) *Cell* **120,** 513–522
31. Noda, A., Ning, Y., Venable, S. F., Pereira-Smith, O. M., and Smith, J. R. (1994) *Exp. Cell Res.* **211,** 90–98
32. Sherr, C. J., and Roberts, J. M. (1995) *Genes Dev.* **9,** 1149–1163
33. Martiny-Baron, G., Kazanietz, M. G., Mischak, H., Blumberg, P. M., Kochs, G., Hug, H., Marme, D., and Schachtele, C. (1993) *J. Biol. Chem.* **268,** 9194–9197
34. Marquez, V. E., and Blumberg, P. M. (2003) *Acc. Chem. Res.* **36,** 434–443
35. Lacal, J. C., Fleming, T. P., Warren, B. S., Blumberg, P. M., and Aaronson, S. A. (1987) *Mol. Cell. Biol.* **7,** 4146–4149
36. Hsiao, W. L., Housey, G. M., Johnson, M. D., and Weinstein, I. B. (1989) *Mol. Cell. Biol.* **9,** 2641–2647
37. Barboule, N., Lafon, C., Chadebech, P., Vidal, S., and Valette, A. (1999) *FEBS Lett.* **444,** 32–37
38. Arita, Y., Buffolino, P., and Coppock, D. L. (1998) *Exp. Cell Res.* **242,** 381–390
39. Frey, M. R., Saxon, M. L., Zhao, X., Rollins, A., Evans, S. S., and Black, J. D. (1997) *J. Biol. Chem.* **272,** 9424–9435
40. Harley, C. B., Futcher, A. B., and Greider, C. W. (1990) *Nature* **345,** 458–460
41. Cozzi, S. J., Parsons, P. G., Ogbourne, S. M., Pedley, J., and Boyle, G. M. (2006) *Cancer Res.* **66,** 10083–10091
42. Niculescu, A. B., 3rd, Chen, X., Smeets, M., Hengst, L., Prives, C., and Reed, S. I. (1998) *Mol. Cell. Biol.* **18,** 629–643
43. Guadagno, T. M., and Newport, J. W. (1996) *Cell* **84,** 73–82
44. Giles, K. M., Daly, J. M., Beveridge, D. J., Thomson, A. M., Voon, D. C., Furneaux, H. M., Jazayeri, J. A., and Leedman, P. J. (2003) *J. Biol. Chem.* **278,** 2937–2946
45. Doller, A., Huwiler, A., Muller, R., Radeke, H. H., Pfeilschifter, J., and Eberhardt, W. (2007) *Mol. Biol. Cell* **18,** 2137–2148
46. Zhou, B. B., and Elledge, S. J. (2000) *Nature* **408,** 433–439
47. Khan, Q. A., and Anderson, L. M. (2001) *Toxicol. Appl. Pharmacol.* **173,** 105–113
48. Zou, Y., Zong, G., Ling, Y. H., Hao, M. M., Lozano, G., Hong, W. K., and Perez-Soler, R. (1998) *J. Natl. Cancer Inst.* **90,** 1130–1137
49. Deng, W. G., Kawashima, H., Wu, G., Jayachandran, G., Xu, K., Minna, J. D., Roth, J. A., and Ji, L. (2007) *Cancer Res.* **67,** 709–717
50. Dangi, S., Chen, F. M., and Shapiro, P. (2006) *Cell Prolif.* **39,** 261–279
51. Esposito, F., Cuccovillo, F., Vanoni, M., Cimino, F., Anderson, C. W., Appella, E., and Russo, T. (1997) *Eur. J. Biochem.* **245,** 730–737
52. Liu, Y., Martindale, J. L., Gorospe, M., and Holbrook, N. J. (1996) *Cancer Res.* **56,** 31–35
53. Ostrovsky, O., and Bengal, E. (2003) *J. Biol. Chem.* **278,** 21221–21231
54. Roninson, I. B. (2003) *Cancer Res.* **63,** 2705–2715
55. te Poele, R. H., Okorokov, A. L., Jardine, L., Cummings, J., and Joel, S. P. (2002) *Cancer Res.* **62,** 1876–1883
56. Krtolica, A., Parrinello, S., Lockett, S., Desprez, P. Y., and Campisi, J. (2001) *Proc. Natl. Acad. Sci. U. S. A.* **98,** 12072–12077